Proceedings of the International Conference on Heat Exchanger Fouling and Cleaning - 2024 (Peer-reviewed)
April 21–26, 2024, Lisbon, Portugal; Editors: H.U. Zettler and E.M. Ishiyama

UNDERSTANDING THE DELIVERY OF ULTRASONIC CLEANING EFFECT IN A HEAT EXCHANGER TUBE

M. Järvinen[1, 2], S. Ahmadzai[1], T. Rauhala[1] and *P. Moilanen[1, 2]
[1] Altum Technologies, Eteläranta 8, 00130 Helsinki, Finland
[2] Electronics Research Laboratory, Physics Department, University of Helsinki, Helsinki, Finland
petro.moilanen@altumtechnologies.com

ABSTRACT

Externally applied online ultrasonic cleaning employs the device's solid structures for the delivery of ultrasound. Since shell and tube heat exchangers (HX) feature complicated structure, we analyze their structural components separately. The present study focuses on single HX tube (model), filled with water and ductile fouling (acrylic resin). Ultrasonic mode analysis based on analytical theory, finite-element simulations and laser Doppler vibrometer experiments are utilized. Ultrasonic cleaning experiments are carried out. At a 20-kHz frequency, flexural wave modes F(1,1) and F(2,1) are actuated. These modes carry ultrasonic energy efficiently along the tube. Since the cavitation threshold is exceeded, sonication at one end permits cleaning of the tube. Cleaning level is shown to depend on distance and cumulative sonication energy. This study provides an important step towards enhancing the externally applied ultrasonic cleaning for HX. Further research is called for evaluating ultrasonic delivery in tubesheet, longer HX tubes, and the impact of shell-side fluid.

INTRODUCTION

Fouling and scaling in industrial systems is a widely known problem. Fouling causes technical challenges basically in the industry as a whole and already in 80s Garret-Price et al. [1] made an extensive report on the problem, economic impact, and techniques on the prevention, mitigation and accommodation of fouling. Specifically in heat exchangers (HX) fouling affects the heat transfer coefficient by increasing the thermal resistance both on the tube and the shell side. Consequently, the fouling also decreases the cross-sectional flow area, which increases the pressure drop across the HX. This increases the work needed by the pumps to keep the same throughput, increasing the electrical power consumption and decreasing the life cycles of the pumps [1].

Traditionally HX are cleaned with hydroblasting which includes blasting the HX with high-pressure water jet. Hydroblasting has several drawbacks: it causes safety risks for the operator, its performance has limitations, it is wasteful in water consumption, and it can damage delicate parts of the machinery. One needs to also take the equipment offline from the process to be able to clean it. This causes production stoppages, decreases in the operation and life cycle of the equipment, further increasing disruptions and the cost of operation. In online scale prevention and fouling mitigation methods, the equipment can be treated while it is in operation. Typically, this is done by addition of chemicals, scale inhibitors or via ion exchange. Not only that can these methods be expensive, but they can also change the chemistry, be inefficient, harsh for environment and harmful for both human and aquatic life [2,3].

Power ultrasound provides a promising alternative for cleaning without high-pressure water jets and harmful chemicals. Ultrasonic cleaning is based on cavitation, which results from the rapid expansion and implosion occurring during the rarefaction and compression phases of the pulsating acoustic pressure field. The collapse of a cavitation bubble creates microjets and shockwaves, both of which can clean solid surfaces. Ultrasonic cleaning is typically carried out in ultrasonic baths. Such solutions are even available for large HX [4]. Advantages of ultrasonic baths compared to hydroblasting include decreased treating duration, enhanced cleaning quality, reduced water consumption and improved operator safety. The major drawback is the requirement for production interruption and offline treatment. Furthermore, the assisting chemicals often required for cleaning may cause issues with some alloys and materials.

To this end, approaches of online ultrasonic cleaning are under active development [5–8]. One of these approaches is the software-guided clamp-on power ultrasonic cleaning method, also known by a brand name Zero-Process-Downtime (ZPD) solution [8]. We recently presented preliminary results on the application of this approach for tubular HX. Our results suggest that the ZPD solution is effective in online fouling prevention, while it can also permit online cleaning. Results on a small-scale laboratory HX were promising. While numerical

ISBN: 978-0-9984188-3-4; Published online www.heatexchanger-fouling.com

simulation predictions were presented also on a full-scale industrial HX, developing the related physical implementation remains as the primary goal. One of the main challenges related to this goal is managing the delivery of ultrasound energy within/across the complex structure of these equipment.

To tackle this challenge, we divide the design task into smaller subtasks, first of which is delivery of ultrasonic cleaning effect in a single HX tube.

An HX tube is essentially an elastic waveguide, filled with and/or surrounded by liquid. Ultrasonic guided waves (GW) are well known and widely used within the non-destructive testing (NDT), i.e. for crack detection or material property evaluation. Guided waves have also been applied to detect scaling in pipelines [9]. Guided waves in a tube wall carry ultrasonic energy over long distances, while at a liquid interface (e.g. liquid inside of the tube), acoustic radiation transforms elastic energy into acoustic pressure energy. In some cases (e.g. tube immersed in surrounding liquid) the acoustic waves do not bounce back into the solid wall, and so-called leaky guided waves are born. Nevertheless, guided waves provide a delivery mechanism for acoustic energy in tubular structures. At high ultrasonic power levels, an ultrasonic cleaning effect based e.g. on cavitation can thus be delivered. In several studies, ultrasonic guided waves were used for descaling pipelines and small scale HX [6,10]. In particular, flexural guided modes have been observed to clean calcium-carbonate fouling in pipes [11].

The objective of this paper is to use ultrasonic mode analysis to determine the guided modes supported by, and actuatable in, a laboratory mimic of a typical HX tube, and to evaluate the feasibility of these modes in preliminary cleaning experiments.

METHODS

Samples

Grade E220-CR2-S3 steel tubes with outer diameter (OD) of 19 mm and wall thickness (WT) of 1.5 mm, meet or exceed the tolerance requirements specified in EN 10305-3 standard. One-meter tubes were used in the cleaning experiments. The tube was chosen since its geometric parameters resemble those of a commercial HXs' tube.

Acrylic resin-based fouling material, available commercially, was used for the fouling of the tubes. The fouling is water resistant when dry i.e. it does not dissolve into the water. The fouling withstands temperatures up to 85 °C. Fouling was applied at the inner surface of the tube wall.

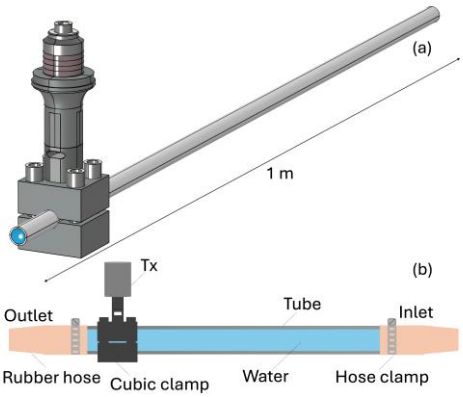

Fig. 1. (a) Geometry of FEM simulations and (b) physical experiments. Inlet and outlet refer exclusively to cleaning experiments. All sonication experiments were done with standing fluid (without flowing).

Ultrasonic mode analysis

A semi-analytical model of ultrasonic modes in a water-filled steel tube was used [12,13]. This model predicted the dispersion curves of acousto-elastic guided waves supported by the tube. The four possible modes are axisymmetric modes L(0,1) and L(0,2) and flexural modes F(1,1) and F(1,2).

Finite-element modelling (FEM) was used to simulate ultrasonic actuation, propagation, and detection in a water-filled steel tube, without and with the fouling. Fouling was mimicked by a 100 µm layer of acrylic resin covering the internal wall. Time-domain simulations were employed using solid mechanics, pressure acoustics and electrostatics modules in COMSOL Multiphysics (version 6.2). Figure 1(a) shows the simulation geometry. A 20 kHz power ultrasound transducer (transmitter) was attached by a sonotrode and a cubical clamp-on mechanism at one end of the tube. Line scan of the normal component of particle velocity was recorded along the tube's long axis, at distances 50 to 350 mm from the transmitter using 5 mm pitch.

In related physical experiments, a laser Doppler vibrometer (LDV; VibroFlex Neo VFX-I-110 with VibroFlex Connect, Polytec GmbH) was employed for the line scan measurement, natively recording the normal component of particle velocity. The LDV line scan ranged from 50 to 350 mm apart from the transmitter with 5 mm pitch. Signals were recorded via PicoScope (Model: 3403D, Pico Technology) attached to the LDV front-end and the conversion factor from LDV was used to convert voltage to meters per seconds. The LDV was attached to a tripod with a traverse stage. The stage was used to move the LDV horizontally between different measurement points. Reflective tape was added to the tube as a diffuser to ease signal capturing.

The recorded spatio-temporal signals was processed by two-dimensional fast Fourier transform, 2D-FFT [12,14] to determine spectral

ISBN: 978-0-9984188-3-4; Published online www.heatexchanger-fouling.com

maxima characteristic of propagating wave modes. Comparison between these spectral maxima against semi-analytical predictions permitted mode identification. Comparison between simulated and experimental 2D-FFT validated the simulated prediction.

MATLAB (R2013a, MathWorks Inc.) was used for semi-analytical modelling and signal processing.

Cleaning experiments

Fouling was manually applied to the tubes and permitted to dry at least 24 hours before sonication. The fouled tube was gently flushed with tap water to let any weakly-attached fouling detach. Rubber hoses were fixed to the inlet and outlet of the tube (Fig. 1(b)) while the hose attached to the inlet was fixed to a water tap. Flushing was done by permitting water to flow freely from the inlet to the outlet, without building up any additional pressure. To ensure that there was no water flow and that the tube was fully filled by water during the sonication experiments; the rubber hoses remained attached to the tube ends by elevating one end of the hose above the tube while keeping the other end attached to the closed tap.

A 20 kHz piezo-electric power ultrasound transducer was used for sonication. The transducer was attached to the tube by a sonotrode and a cubic clamp-on coupler. The coupler was attached to the tube so that its middle point was approximately 100 mm away from the tube outlet.

The ultrasonic transducer was sonicated by the commercially available ZPD solution of Altum Technologies, using pulsed actuation waveforms. During an individual sonication experiment, the sonication power remained constant, however, it was adjusted between the experiments.

Table 1 summarizes the experiments carried out, for three tube samples featuring similar fouling layer applied at their inner surface. Tube sample #1 was inspected five times during the sonication, with varying intervals. This permitted evaluation of the cleaning progress and iterative adjusting of the sonication power level. The remaining tube samples #2 and #3 were sonicated without interruption until inspection.

Sonication time and the electrical power as a function of time were logged for each sonication experiment. The cumulative sonication energy (ΣE) was calculated by integrating the power with respect to (wrt.) time and multiplying the result with the used duty cycle. Cavitation was detected in the tube as a broadband noise using LDV spectral assessment [15] when electrical power was 70 W or higher.

The temperature of the ultrasonic coupler was monitored by a temperature sensor (PT100) during the 4-hour and the two 13-hour cleaning experiments. It was observed that the temperature did not exceed 65 °C.

Table 1. Summary of cleaning experiments, including sample number (#) sonication power ($\bar{P}$) (average ± standard deviation), sonication duration (ΔT) and cumulative sonication energy (ΣE).

#	$\bar{P}$ [W]	ΔT [h]	ΣE [MJ]
1	104 ± 4	1	0.1
1	105 ± 6	2	0.3
1	203 ± 12	1	0.5
1	203 ± 11	1	0.6
1	347 ± 22	4	1.9
2	198 ± 40	13	2.2
3	197 ± 18	13	2.1

The tubes were inspected for cleaning level (CL) by imaging, using a commercially available endoscope. The inspection was done after flushing the tube with water and after each sonication experiment. Images (resolution 640 x 480; 8 bits) were taken from the inlet towards the outlet. The first picture was taken at about 800 mm distance from the center of cubic coupler. Pictures were taken at approximately 50 mm intervals while ensuring that the fouling was not damaged in the process. To ensure a similar camera position between pictures the endoscope was fitted with plastic cylinder increasing its OD to 15 mm.

The endoscope image wrt. distance data set was analyzed with a custom script written with Python (version 3.6.11) programming language. The images were segmented using thresholding, to create binary images. In the binary image, 1 (visualized e.g. by white color) represents fouling, and 0 (visualized e.g. black color) represents cleaned surface. A cleaning level (CL) was then determined by

$$CL = 1 - \frac{\sum_{i=1}^{n}\sum_{j=1}^{m} B_{i,j}}{n*m-\pi r^2},\ CL \in [0,1], \qquad (1)$$

where $B_{i,j}$ denotes the binary image pixel value, r is the tubes center radius (set to be 80 pixels), n and m are the rows and columns of the binary image respectively. Note that CL is an areal quantity. When CL is zero, it is interpreted that the image contains only fouling, while when CL is one the interpretation is that only metal is seen in the picture.

The threshold level was manually set for each image by identifying exposed metal and selecting the brightest area from it, at most 15x15 pixels. From this area the highest pixel intensity was selected. This was deemed to be the highest pixel intensity value for the metal surface in the image. For an additional safety margin, to avoid false classification of metal as fouling, an arbitrary value of 5 intensity levels was added onto the threshold level.

To smoothen noise, due to segmentation uncertainty, in the experimental CL wrt. ΣE data, a

ISBN: 978-0-9984188-3-4; Published online www.heatexchanger-fouling.com

moving average filter featuring a window of 3 samples was applied.

A functional relation between the cumulative sonication energy Σ*E* and the cleaning level *CL* can be expressed by

$$CL(\Sigma E) = a(\Sigma E)^{\gamma} + b, \quad \gamma \in [0, 1], \qquad (2)$$

where γ, a and b are three unknown parameters. This model (Eq. 2) was fitted with experimentally measured *CL* wrt. Σ*E* data by using a nonlinear least-squares algorithm.

RESULTS

Ultrasonic mode analysis

Figure 2 illustrates the total displacement field generated by power ultrasound actuation (200W, 20.6 kHz) in the water-filled tube. The displacement field is well carried along the 1 m long tube. The displacement shape exhibits the characteristics of flexural modes, F(1,1) and F(2,1). Features of axisymmetric propagation was not observed.

Figure 3(a) shows the 2D-FFT mode map generated from the simulated line scan. There are two intensity maxima observed, centered at the sonication frequency (20.6 kHz), and their spectral peak positions are well consistent with the theoretically predicted phase velocities of F(1,1) and F(2,1) modes.

Figure 3(b) shows related 2D-FFT mode map generated from the LDV line scan, measured in a real water-filled tube. The interpretations are mainly consistent with those made from simulations, with the exception that the real transducer featured a slightly higher (+1.5 kHz) tuning frequency when coupled onto the tube, and the magnitude ratio of the spectral maxima is slightly different compared to simulated predictions. Nevertheless, the F(1,1) and F(2,1) modes consistently explain the wave propagation in both the predicted and physical experiments.

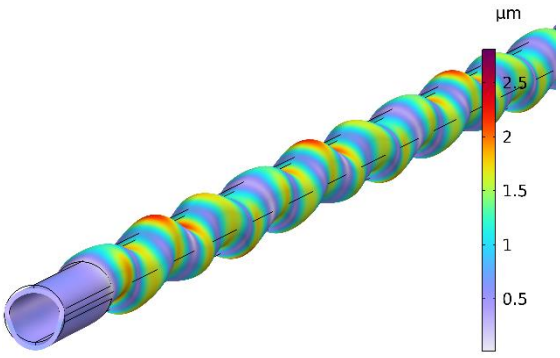

Fig. 2. Temporal snapshot (*t* =4 ms) of the simulated ultrasonic displacement field propagating in the wall of a water-filled tube. The ultrasonic clamp-on transducer (not shown) is located on the left. The tube was sonicated by a 200W (avg) power.

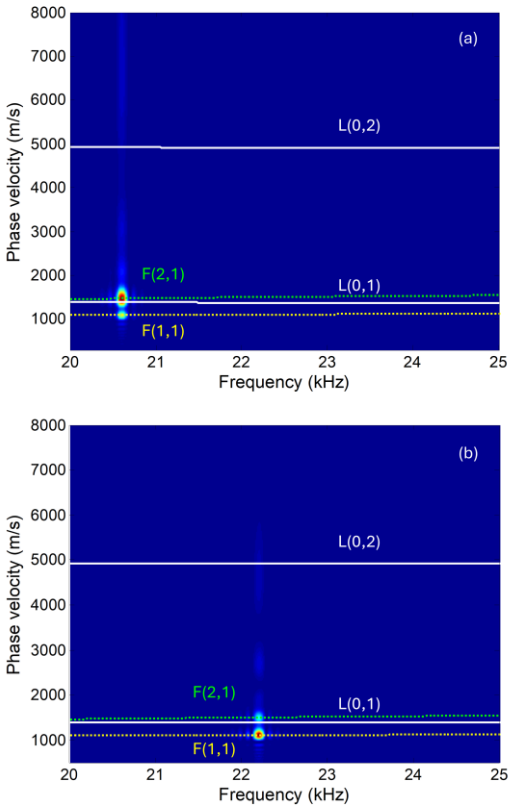

Fig. 3. 2D-FFT mode maps of (a) the simulated and (b) the experimental line scan. Semi-analytical predictions are shown by lines superimposed.

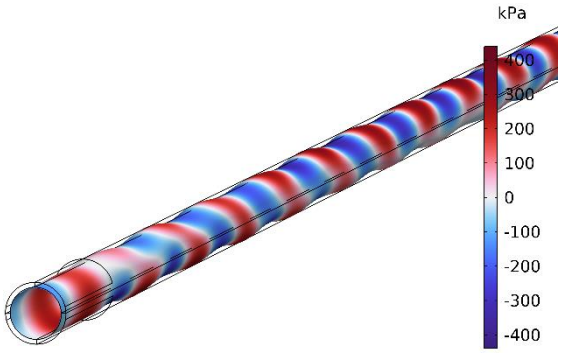

Fig. 4. Temporal snapshot (*t* =4 ms) of the simulated acoustic pressure field generated into the water column by a 200W (avg) sonication power.

Figure 4 shows the propagating acoustic pressure field generated into the water column of the tube by power ultrasound actuation (200W, 20.6 kHz).

Cleaning experiments

Figure 5 shows endoscope images at *D* = 550 mm distance from the ultrasonic transducer, before and after sonication (cumulative sonication energy Σ*E* = 1.9 MJ). Bottom panel shows the segmented images, with white color representing fouling and black color representing cleaned surface. Clear impact of reduced fouling due to sonication can be

ISBN: 978-0-9984188-3-4; Published online www.heatexchanger-fouling.com

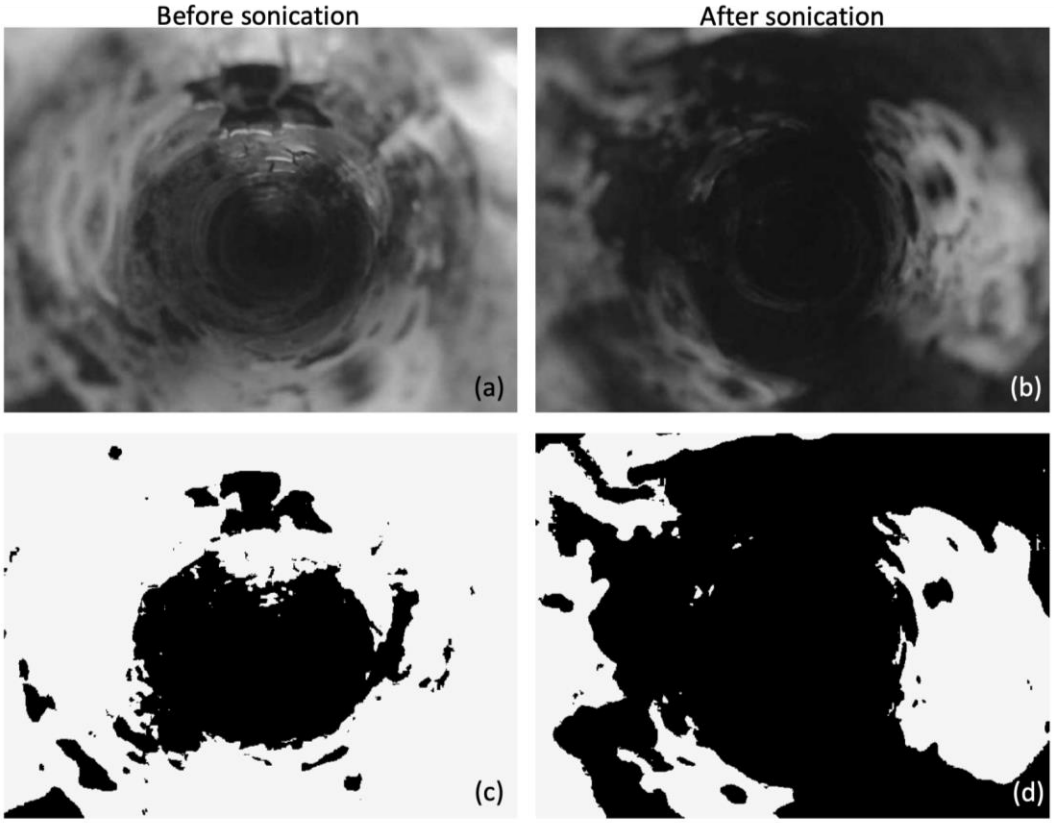

Fig. 5. Endoscope images taken (a) before sonication and (b) after sonication (ΣE = 1.9 MJ, sample number 1), at distance D = 550 mm from the ultrasonic transducer. Related segmented images (c) before sonication and (d) after sonication show fouling by white color and clean tube by black color.

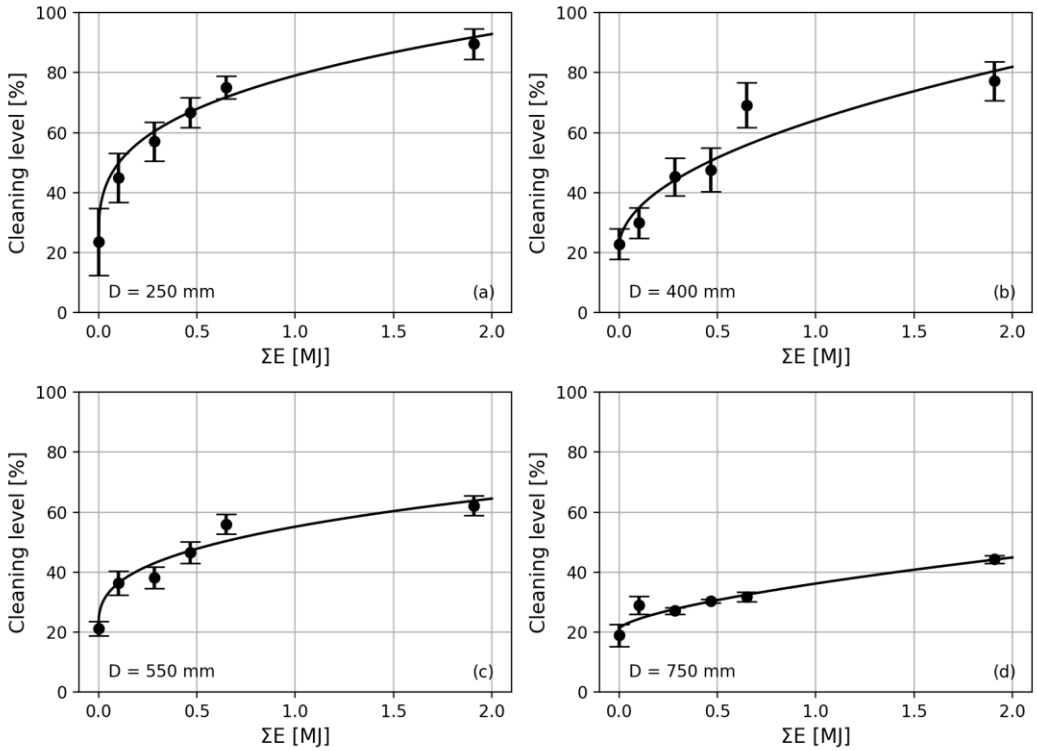

Fig. 6. Cleaning level as a function of cumulative sonication energy (ΣE, solid markers), determined at the distances of (a) D = 250 mm, (b) 400 mm, (c) 550 mm and (d) 750 mm. Error bars represent

ISBN: 978-0-9984188-3-4; Published online www.heatexchanger-fouling.com

repeatability of the endoscope imaging. Solid curves represent the theoretical model (Eq. 2) fitted on the experimental data.

seen by the increased area of black pixels, although the imaged tube section is not yet totally clean. Afterwards when the pipes were flushed, the fouling was mainly observed to be dissolved in the water, though some fouling flakes were still present.

Figure 6 shows the cleaning level as a function of cumulative energy for several transducer-to-camera distances *D*. The shape of the cleaning response depends on the distance *D*. When close to the ultrasonic transducer (*D* = 250 mm) the response is nonlinear (γ = 0.3), whereas when far (*D* = 750 mm, γ = 0.65) the response approaches a linear curve (γ = 1). Importantly, the cleaning rate (i.e. $\Delta CL/\Delta\Sigma E$) and the achieved cleaning level depends on *D*. The cleaning rate is higher near the transducer and decreases with increasing distance from it. We can also observe that the cleaning rate slows down as the cumulative sonication energy Σ*E* increases. For instance, as shown in Fig. 6(a), more cumulative energy is needed to progress from *CL* = 80% to *CL* = 90% compared to the cumulative energy needed to progress from *CL* = 20% to *CL* = 80%.

Figure 7 shows the cleaning level wrt. transducer-to-camera distance *D* for the maximal cumulative energy Σ*E* (approximately 2.1 MJ) delivered on the three successive experiments. The results suggest excellent cleaning, *CL* > 90%, within the proximity (*D* ≤ 250 mm) of the ultrasonic transducer. When moving further away from it (*D* > 250 mm), *CL* decreases gradually, approximately -0.7 to -1 %-unit per 10 mm, being *CL* = 40% at distance *D* = 800 mm.

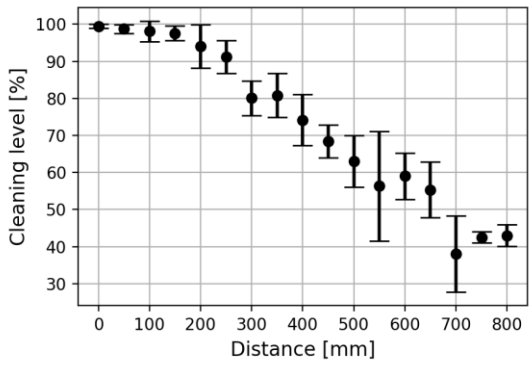

Fig. 7. Cleaning level as a function of ultrasonic-transducer-to-camera distance *D* for the average cumulative energy of Σ*E* = 2.1 MJ. Markers show the average of three repeated experiments and error bars the standard deviation.

DISCUSSION

In this study it was shown that we can predict the ultrasonic wave modes that are produced by 20 kHz power ultrasound actuation, and that these modes permit efficient delivery of ultrasonic cleaning effect in tubes resembling those found in a shell and tube HX. In particular, the modes were characterized as the flexural guided modes, F(1,1) and F(2,1), of a liquid-filled tube. It was predicted by FEM simulations, that a 200W sonication power results in acoustic pressure field inside the tube, which is sufficient to exceed the cavitation threshold. Thus, cavitation was regarded as the major cleaning mechanism. Cleaning level was shown to depend on cumulative sonication energy, and an empirically determined power function was shown to fit well the measured cleaning level data. This suggests that the cleaning effect may be well predictable and could potentially be managed by adjusting sonication parameters such as power, duty cycle and duration. While the cleaning efficiency was shown to decrease with sonication distance, our results clearly indicate that the tube would eventually be cleaned when enough energy is delivered.

The experimental results suggest that the cumulative energy transferred to the tube is a crucial parameter for cleaning. The functional form in figure 6 suggests that there might be two distinct physical mechanisms involved in cleaning, one due to high displacement amplitudes near the transducer, and one due to acoustic cavitation. Another important parameter is the temperature. The temperature of the cubic coupler was measured, and though it did not exceed 65 °C (85 °C is the quoted limit of the fouling) it heated the water inside the tube. This warmed up the water near the cubic coupler (transducer). Due to this, cavitation might have occurred more easily near the cubic coupler, via increase in vapor pressure. In the literature water's cavitation threshold level has been shown to decrease with increasing temperature [16] while also the raised temperature may enhance ultrasonic cleaning [17]. As such, cavitation together with the higher amplitudes near the transducer could result in a higher cleaning rate. First, high displacements and cavitation break the adhesion until a certain threshold level in CL is achieved. Second, cavitation remains the main cleaning mechanism which results in a lower relative cleaning rate. Still, we can observe some non-linearity (γ < 1) at 750 mm distance from the transducer, where the temperature rise was negligible. This implies that even at this distance, two distinct phenomena may be in play.

The choice of using commercially available acrylic resin as a fouling mimic is worth elaborating upon. We chose this type of fouling intentionally due to its ductile properties, while limescale more generally used for scaling mimic is brittle. We have also observed that with limescale the drying time is a crucial parameter. If the drying time is too short the scaling is rather easy to detach, while on the other hand, if the scaling has remained on a surface

ISBN: 978-0-9984188-3-4; Published online www.heatexchanger-fouling.com

for an extensive period, it becomes very hard to remove. The limescale's adhesion strength is dependent on the surface properties and cleanliness. Also applying thin layers consistently needs specially built contraptions. Compared to this, the acrylic-resin fouling allows quicker iterations and due to its viscoelastic (ductile) properties, it should be harder for ultrasound to remove.

The mode analysis and simulation results show that modes generated in the tube are not dispersive i.e. the phase velocity is relatively constant within the frequency range of interest (20-25 kHz). This suggests that modal coupling does not significantly depend on the sonication frequency within this range, like it often does on related applications of guided waves. The predicted negative acoustic pressure amplitude (Fig. 3) exceeds the atmospheric pressure by approximately threefold at a 200W sonication power. Hence, the results predict that cavitation will occur inside the tube at power levels considered in this study. This is also supported by the experimental work.

A limitation of the image analysis method used is the introduction of human bias when selecting the threshold value. Still, we tried to be as consistent as possible when choosing the threshold value. Automatic thresholding algorithms, such as Otsu's method, were considered, but they did not work well with our image data. The main issues are that all our images do not have a clear bimodal distributed histogram, the data itself is noisy, and lighting is inhomogeneous. Due to this, we decided to individually threshold each image and to accept the possible human bias. Another limitation in the analysis is the projection of 3D cylinder shape onto a two-dimensional plane. Thus, the metric equivalence of one endoscope image pixel varies with the respective axial position within the image. Due to this perspective, features near the lens appear bigger than related features further away from it. Consequently, cleaning level is more sensitive to features near the lens than those far away. Hence the cleaning level is essentially measured only near the lens. Note that this error is smallest when the cleaning level is 100 % or 0 %. Nevertheless, even with its limitations the cleaning level was deemed to be representative for the purpose.

The increase of cleaning level with cumulative energy when D = 750 mm from the transducer implies that both the sonication power and duration play a role. This suggests that by using a combination of sufficient power and sufficient duration, the entire tube can be cleaned. Regarding this, a study by Herbert et al. [18] showed that the cavitation threshold probability is not a step function but rather an S-curve. Also, the literature does not typically represent the cleaning levels wrt. cumulative sonication energy. Rather only sonication duration and sonication power levels are quoted. Calculating the cumulative energy has advantages since it provides tangible energy cost for the cleaning treatment. For instance, 2.1 MJ equals approximately 0.58 kWh, and with e.g. the price of 10 euro cents per kWh this results in a 5.8 euro cents cost for the cleaning treatment.

The successive cleaning experiments (Fig. 7) represent good repeatability. The error bars are mainly explained by uncertainties in camera position parameters, namely transducer-to-camera distance, and camera orientation. Variations in the quality of mechanical coupling with the cubic clamp-on device may also have an effect. Moreover, small fluctuations in $\bar{P}$ and ΔT biases in predicted ΔT during the 13h experiments cause some variability in the cumulative sonication energy. This variability, modulated by the functional relationship between distance D and cumulative energy ΣE, is reflected in the error bars seen in Figure 7.

The trend of the CL wrt. D relation (Fig. 7) suggest a decay with distance and, at short distances, asymptotic approaching of the 100% cleaning level. From the behavior of this spatial decay function a question arises about the reach of the cleaning effect in realistic HX tubes, which typically feature lengths of several meters. In this preliminary study we tested the concept of fouling removal experiments in 1 m long tubes. The results seem reproducible and reflect the trends of underlying physical mechanisms, thereby supporting continuation of the experimental work for a more thorough understanding. Similar experiments in longer (e.g. 6 m long) tubes would give a more realistic picture of the design constraints of real industrial scale HX.

While the present experimental setup with single ultrasonic transducer aims to model the configuration of ultrasonic actuation at one HX tubesheet, attaching another transducer onto the opposite end of the tube sample would respectively model the configuration of ultrasonic actuation at two tubesheets. Beam steering, e.g. by phased excitation, would in this case permit controlled magnification and translation of the cleaning effect within the tube. This approach may well be essential for the success while operating at full industrial length scales. U-tube HX, such as those discussed in [8], permit the same via sonicating their one and only tubesheet.

The tube model (sample) featured a smooth surface, while real HX tubes often have surface texture. The dimension of typical texture is much smaller than the wavelengths (a few centimeters) characteristic to the flexural modes discussed here, hence such structural features are not expected to cause significant disturbance to the propagation of ultrasonic wave modes. They can, however, affect the cleaning effect by disturbing cavitation. Petkovšek et al. showed that microstructure could affect cavitation induced by fluid flow [19], as such we expect cavitation induced by ultrasound to be

ISBN: 978-0-9984188-3-4; Published online www.heatexchanger-fouling.com

affected as well. Nevertheless, further research is needed to address this question.

In this study we focused on analyzing the impact of tube side liquid and fouling at the tube side. Related properties of shell-side liquid and fouling should be addressed by further research.

CONCLUSION

This study features the first fundamental step towards enhancing the application of software-guided clamp-on power ultrasonic cleaning on full industrial scale shell and tube HX. Our results suggest that ultrasonic cleaning of an individual HX tube is viable by moderate sonication power levels. The next design step should focus on optimizing ultrasonic delivery within the tubesheet, by using beam steering algorithms and an array of ultrasonic transducers. Focusing ultrasonic energy into a chosen tube within the tube bundle permits a source for ultrasonic cleaning within this tube. The results of the present study will then become valuable.

The final implementation will have a significant impact on the industry. While the present study discussed primarily ultrasonic cleaning, the same technology will provide its best value on scaling and fouling prevention. The prevention permits maintaining the heat exchanger efficiency and thereby provides economic, environmental and financial benefits as compared to a more traditional approach based on cleaning cycles. Therefore, fouling prevention with the software-guided clamp-on power ultrasound solution is ideal for the industry.

NOMENCLATURE

D	Transducer-to-camera distance, mm
CL	Cleaning level, dimensionless
ΣE	Cumulative sonication energy, J
$\bar{P}$	Sonication power (real average), W
ΔT	Sonication duration, h
γ	exponent coefficient (Eq. 2), dimensionless
a	linear coefficient (Eq. 2), $1/J^{\gamma}$
b	intercept coefficient (Eq. 2), dimensionless
r	Radius of the center of the tube, pixels
$B_{i,j}$	Binary image pixel value, dimensionless
n	rows of the binary image, dimensionless
m	columns of the binary image, dimensionless

REFERENCES

[1] Garrett-Price, B. A., Smith, S. A., and Watts, R. L., *Industrial Fouling: Problem Characterization, Economic Assessment, and Review of Prevention, Mitigation, and Accommodation Techniques*, Pacific Northwest National Lab.(PNNL), Richland, WA (United States), 1984.

[2] Naddeo, V., Borea, L., and Belgiorno, V., Sonochemical Control of Fouling Formation in Membrane Ultrafiltration of Wastewater: Effect of Ultrasonic Frequency, *Journal of water process engineering*, vol. 8, pp. e92–e97, 2015.

[3] Jafari, M., D'haese, A., Zlopasa, J., Cornelissen, E. R., Vrouwenvelder, J. S., Verbeken, K., Verliefde, A., van Loosdrecht, M. C. M., and Picioreanu, C., A Comparison between Chemical Cleaning Efficiency in Lab-Scale and Full-Scale Reverse Osmosis Membranes: Role of Extracellular Polymeric Substances (EPS), *Journal of Membrane Science*, vol. 609, p. 118189, 2020.

[4] Shank, R. A., and McCartney, T. R., Simultaneous Effective Removal of Polysulfide and Polyolefin Fouling from Twisted Tube®® Heat Excangers in Hydrocracker Process Using Ultrasonic Chemical Cleaning, 2022.

[5] Lais, H., Lowe, P. S., Gan, T.-H., and Wrobel, L. C., Numerical Investigation of Design Parameters for Optimization of the In-Situ Ultrasonic Fouling Removal Technique for Pipelines, *Ultrasonics Sonochemistry*, vol. 56, pp. 94–104, 2019.

[6] Kamar, N., Scaling Control by Using Ultrasonic Guided Waves, *Chemical Engineering and Processing - Process Intensification*, vol. 176, p. 108969, 2022.

[7] Banakar, V. V., Gogate, P. R., Raha, A., and Saurabh, Application of Ultrasound in Heat Exchanger Handling Supersaturated CaSO4 Solution for Reduction of Scaling by Induced Precipitation and In-Situ Cleaning, *Chemical Engineering Science*, vol. 276, p. 118814, 2023.

[8] Moilanen, P., Rauhala, T., and Ahmadzai, S., Software-Guided Clamp-on Power Ultrasound Solution for Fouling Mitigation in Tubular Heat Exchangers, *Heat and Mass Transfer*, 2023.

[9] Lais, H., Lowe, P. S., Gan, T.-H., Wrobel, L. C., and Kanfoud, J., Characterization of the Use of Low Frequency Ultrasonic Guided Waves to Detect Fouling Deposition in Pipelines, *Sensors*, vol. 18, no. 7, p. 2122, 2018.

[10] Qu, Z., Yang, J., Wu, L., An, Y., Liu, Y., Yin, W., Jin, S., Yang, X., Wang, Q., and Fang, R., Methodology for Removing Fouling within Liquid-Filled Pipelines Based on Ultrasonic Guided Waves Cavitation Effect, *Applied Acoustics*, vol. 157, p. 107018, 2020.

[11] Nakagawa, N., Fujihara, M., Wu, C., and Satonobu, J., Removal of Pipe Fouling inside Pipes Using Ultrasonic Waves, *JSME International Journal Series C Mechanical Systems, Machine Elements and Manufacturing*, vol. 49, no. 3, pp. 713–718, 2006.

ISBN: 978-0-9984188-3-4; Published online www.heatexchanger-fouling.com

[12] Moilanen, P., *Ultrasonic Guided Wave Measurements in Bone*, Ph.D. thesis, University of Jyväskylä, 2004. (thesis)
[13] Pavlakovic, B. N., Leaky Guided Ultrasonic Waves in NDT, Ph.D. thesis, University of London, 1998. (thesis)
[14] Alleyne, D., and Cawley, P., A Two-Dimensional Fourier Transform Method for the Measurement of Propagating Multimode Signals, *The Journal of the Acoustical Society of America*, vol. 89, no. 3, pp. 1159–1168, 1991.
[15] Promasa, K., Non-Invasive Measurement Techniques to Monitor Acoustic Cavitation Activity, Ph.D. thesis, University of Strathclyde, 2014. (thesis)
[16] Magaletti, F., Gallo, M., and Casciola, C. M., Water Cavitation from Ambient to High Temperatures, *Scientific Reports*, vol. 11, no. 1, p. 20801, 2021.
[17] Huang, M., Han, C., An, Y., Qu, Z., Chen, C., and Yin, W., Influence of Temperature on Fouling Removal for Pipeline Based on Eco-Friendly Ultrasonic Guided Wave Technology, *Clean Technologies and Environmental Policy*, vol. 25, no. 4, pp. 1211–1221, 2023.
[18] Herbert, E., Balibar, S., and Caupin, F., Cavitation Pressure in Water, *Physical Review E*, vol. 74, no. 4, p. 041603, 2006.
[19] Petkovšek, M., Hočevar, M., and Gregorčič, P., Surface Functionalization by Nanosecond-Laser Texturing for Controlling Hydrodynamic Cavitation Dynamics, *Ultrasonics Sonochemistry*, vol. 67, p. 105126, 2020.

ISBN: 978-0-9984188-3-4; Published online www.heatexchanger-fouling.com